JACS
JOURNAL OF THE AMERICAN CHEMICAL SOCIETY

COMMUNICATION

pubs.acs.org/JACS

Transformative Two-Dimensional Layered Nanocrystals

Sohee Jeong,[†] Jae Hyo Han,[†] Jung-tak Jang,[†] Jung-wook Seo,[†] Jin-Gyu Kim,[‡] and Jinwoo Cheon*[,†]

[†]Department of Chemistry, Yonsei University, Seoul 120-749, Korea

[‡]Division of Electron Microscopic Research, Korea Basic Science Institute, Daejeon 305-333, Korea

Supporting Information

ABSTRACT: Regioselective chemical reactions and structural transformations of two-dimensional (2D) layered transition-metal chalcogenide (TMC) nanocrystals are described. Upon exposure of 2D TiS_2 nanodiscs to a chemical stimulus, such as Cu ion, selective chemical reaction begins to occur at the peripheral edges. This edge reaction is followed by ion diffusion, which is facilitated by interlayer nanochannels and leads to the formation of a heteroepitaxial TiS_2-Cu_2S intermediate. These processes eventually result in the generation of a single-crystalline, double-convex toroidal Cu_2S nanostructure. Such 2D regioselective chemical reactions also take place when other ionic reactants are used. The observations made and chemical principles uncovered in this effort indicate that a general approach exists for building various toroidal nanocrystals of substances such as Ag_2S, MnS, and CdS.

Nanoscale chemical reactivity forms an important basis for many characteristics of nanomaterials ranging from catalytic efficiency to structural transformations.[1] Recently, 2D layered nanomaterials, such as graphene analogues and transition-metal chalcogenides (TMCs), have attracted significant interest from theory to material synthesis and device fabrication.[2,3] The structural characteristics of 2D TMC nanomaterials, including the anisotropy associated with the large aspect-ratio differences between edges and planes and the weakly interacting layered structure that enables intercalation,[3a−e] have been actively investigated. However, the solid-state chemical reactivity of these materials remains relatively unexplored.[4]

In the study described herein, we have uncovered a unique regioselective anisotropy of 2D layered TMCs that governs the initial chemical reactivity and subsequent structural evolution processes. As shown in Figure 1a, conventional shape-transformative reactions of spherical nanocrystals usually lead to the formation of hollow nanostructures having concavo-convex curvature.[5] In contrast, we have discovered that layered 2D structures behave differently in transformative processes in that they give structurally unique double-convex curvature (Figure 1b). This phenomenon is driven by the existence of regioselective edge reactions and ion migration through nanochannels between the layers.

The morphology resulting from these processes is a toroid (Figure 1c), a basic, highly symmetric, double-convex geometrical structure with a hole in its center like a doughnut.

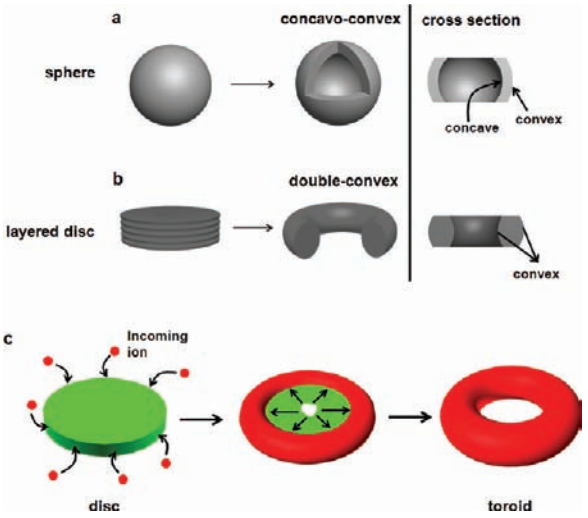

Figure 1. Void curvatures in transformed nanocrystals. (a) Concavo-convex curvature from a sphere to a hollow sphere. (b) Double-convex curvature from a layer-structured disc to a toroid. (c) Schematic illustration of 2D layered nanocrystals reacting with incoming ions regioselectively to form a toroid as the final product.

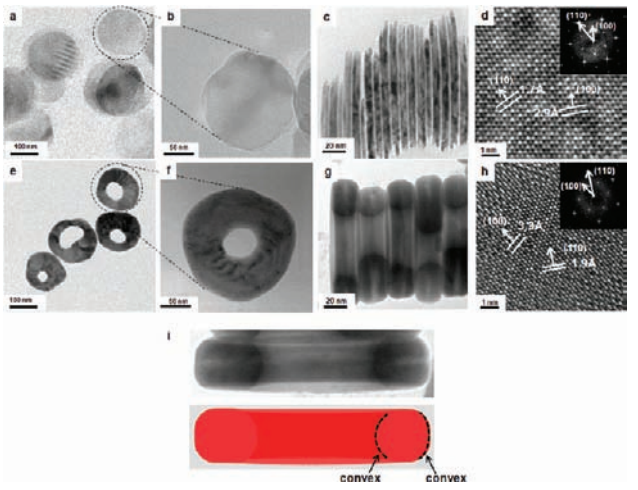

Figure 2. TEM images of TiS_2 discs and transformed Cu_2S toroids. (a, b) Low-resolution and magnified images of TiS_2 disc nanocrystals (c) Side view of TiS_2 discs stacked together. (d) HRTEM image and (inset) FFT pattern of TiS_2. (e, f) Low-resolution and magnified images of Cu_2S toroids. (g) Side view of Cu_2S toroids stacked together. (h) HRTEM image and (inset) FFT pattern of Cu_2S. (i) TEM image and schematic drawing of a Cu_2S toroid exhibiting double-convex curvature.

Received: May 30, 2011
Published: August 29, 2011

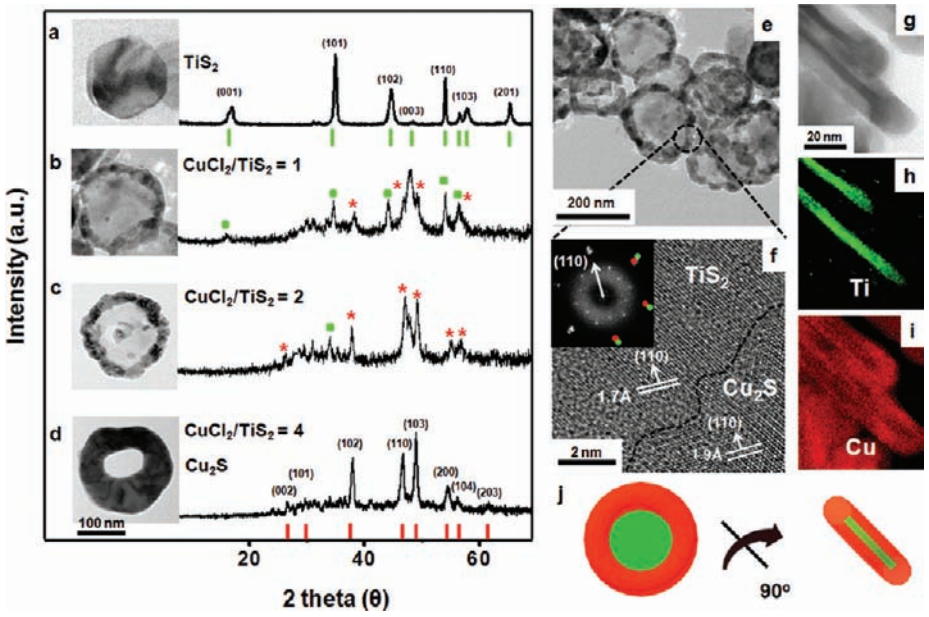

Figure 3. TEM images and XRD patterns of transformative nanostructures reflecting the effects of Cu ion on TiS_2. (a) TEM image and XRD pattern of a pure TiS_2 nanodisc. (b−d) TEM images and XRD patterns from structures obtained by reactions carried out at different molar ratios of reactants: (b) $CuCl_2/TiS_2 = 1$; (c) $CuCl_2/TiS_2 = 2$; (d) $CuCl_2/TiS_2 = 4$. In the XRD patterns, the green squares and red stars represent peaks from TiS_2 and Cu_2S, respectively. (e) Large-area image of the intermediate TiS_2-Cu_2S structure obtained with $CuCl_2/TiS_2 = 1$. (f) High-magnification image at the interface between TiS_2 and Cu_2S showing that the (110) planes of Cu_2S with a 1.9 Å lattice fringe are oriented in the same direction as the (110) planes of TiS_2 with a 1.7 Å lattice fringe. The FFT pattern (inset) shows green and red dots corresponding to TiS_2 and Cu_2S, respectively. (g−i) Side-view TEM image (g) and EELS elemental analysis (h, i) of an intermediate TiS_2-Cu_2S structure. Ti is shown in green and Cu in red. (j) Schematic rotation of the intermediate structure by 90°, showing both planar and side-view images.

Because of their unique shape, toroids have been observed to exhibit unusual optical[6] and magnetic properties.[7] Although toroidal structures in the bulk or micrometer-size regime have been fabricated,[8] their nanoscale structures have been rarely observed.[9]

With the aim of exploring the synthetic accessibility of nanoscale toroidal structures through the use of transformative reactions, we prepared 2D disc-shaped TiS_2 nanocrystals consisting of S−Ti−S layers stacked in the ⟨001⟩ direction. The TiS_2 nanodiscs were generated by adding carbon disulfide (CS_2) to a mixture of titanium(IV) chloride and oleylamine at 300 °C. Transmission electron microscopy (TEM) analysis (Figure 2a−d) reveals that TiS_2 produced in this manner is a single crystalline disc having a diameter of 150 nm and a thickness of 10 nm with lattice fringes of 2.9 Å for the (100) planes and 1.7 Å for the (110) planes. Its single crystallinity was further confirmed by the regular hexagonal patterns seen in the fast Fourier transform (FFT) of a high-resolution TEM (HRTEM) lattice image (Figure 2d inset) and an electron diffraction (ED) pattern (Figure 4k).

The nanodiscs were used as a template for chemical transformations. $CuCl_2$ was added to TiS_2 nanodiscs in oleylamine, and the mixture was heated at 200 °C for 30 min. During this process, the initial blue-black solution turned to a brown color, and the product was then precipitated by adding a mixture of *n*-butanol and hexane. TEM analysis (Figure 2e−h) indicates that the product has a toroidal morphology. The exterior diameter of the toroids is 160 nm, and the ring thickness is 31 nm (Figure 2e−g). Elemental analysis using electron energy loss spectroscopy (EELS) and X-ray diffraction (XRD) confirm that the toroidal nanocrystals are comprised of pure Cu_2S (Figure S1 in the Supporting Information). The results show that the single-crystalline toroid has lattice fringes of 3.3 and 1.9 Å (Figure 2h), which are consistent with the (100) and (110) planes of Cu_2S and the hexagonal pattern of the FFT (Figure 2h inset). A side view of the Cu_2S toroid indicates that it possesses double-convex curvature (Figure 2i).

These chemical transformation processes are highly sensitive to reaction conditions such as the temperature, time, and stoichiometry of the reactants. For example, at lower temperature (100 °C), no significant chemical or morphological transformation occurs. However, at 200 °C, time-dependent morphological changes are clearly observed (Figure S2). When the molar ratio of Cu ion to TiS_2 is 2:1, nucleation of Cu_2S was observed on the edges of the discs within 30 min. After 1 h, small voids gradually appear in the center of the discs, and within 2 h, enlarged voids are apparent and the toroidal Cu_2S structure is produced. However, under these conditions, the formation of a well-defined and single-crystalline toroidal structure is not optimized.

To achieve a completely transformative reaction, the amount of reactant molecule relative to the template nanocrystal is important. Using TEM and XRD, we monitored the dependence of these transformative reactions on the amount of reactant at 200 °C for 30 min (Figure 3a−d). When the molar ratio of Cu ion is low ($CuCl_2/TiS_2 = 1$), darkened regions indicating Cu_2S formation are confined primarily to the edges of the TiS_2 (see the TEM image in Figure 3b). Simultaneously, peaks from Cu_2S (red ★ in Figure 3b) are seen along with peaks of TiS_2 (green ■) in the XRD pattern.[10] As the $CuCl_2/TiS_2$ ratio is increased to 2, the thickness of the dark-contrast edge region increases in the TEM image and the intensities of the XRD peaks associated with Cu_2S become larger (Figure 3c). Eventually, when the $CuCl_2/TiS_2$ ratio is increased to 4, the transformation

dx.doi.org/10.1021/ja2049594 |*J. Am. Chem. Soc.* 2011, 133, 14500–14503

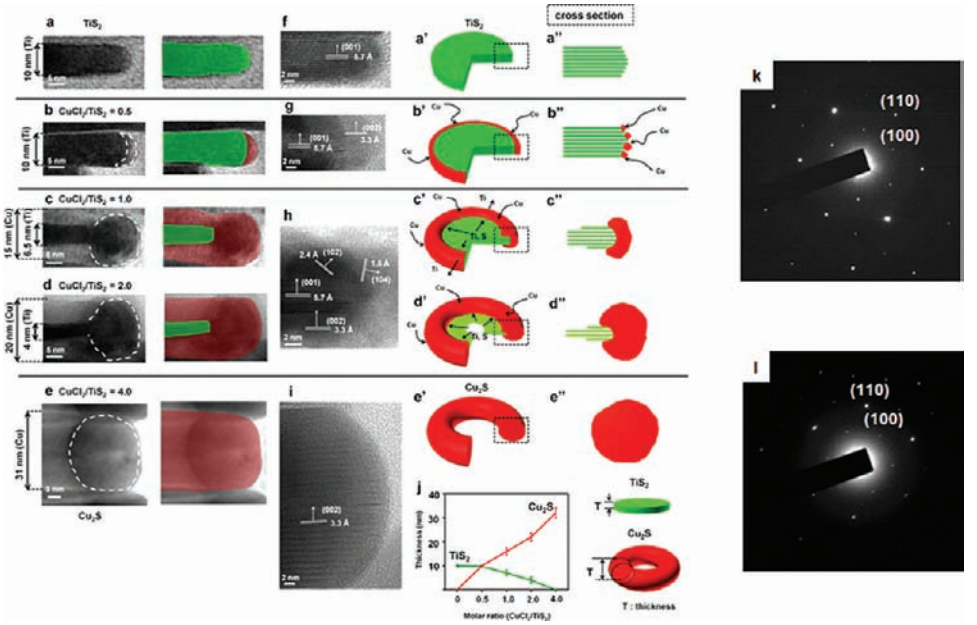

Figure 4. Side-view TEM images and structural changes from 2D discs to toroids. (a−e) TEM images of nanostructures obtained from reactions carried out with different ratios of Cu ion ($CuCl_2/TiS_2$ = 0, 0.5, 1, 2, and 4). The right-hand TEM images are false-colored as pink for Cu_2S and green for TiS_2 for clear visibility. The white dashed lines present the formation of the double-convex curvature of Cu_2S. (f) HRTEM image of layered TiS_2 with lattice fringes of 5.7 Å corresponding to the (001) plane. (g) HRTEM image of the structure obtained with $CuCl_2/TiS_2$ = 0.5. The (002) planes of Cu_2S are oriented parallel to the (001) planes of TiS_2. (h) HRTEM image of the structure obtained with $CuCl_2/TiS_2$ = 1. The (001) planes of TiS_2, (002) planes of Cu_2S, and Cu_2S layers elongated along the ⟨102⟩ and ⟨104⟩ directions with lattice fringes of 2.4 and 1.5 Å, respectively, are shown. (i) HRTEM image of the structure obtained with $CuCl_2/TiS_2$ = 4, showing single-crystalline Cu_2S with (002) lattices of 3.3 Å. (a′−e′) Schematic diagrams of the transformation of TiS_2 discs to Cu_2S toroid structures via TiS_2−Cu_2S intermediates. (a″−e″) Cross-sectional views of (a′−e′). Green represents TiS_2 and red Cu_2S. (j) Plot showing the change in thickness of TiS_2 and Cu_2S with increasing $CuCl_2/TiS_2$ ratio. (k, l) ED patterns of TiS_2 and Cu_2S, respectively. Both ED patterns indicate single crystallinity.

to a toroidal shape becomes complete, as shown by the observation that the peaks in the XRD pattern corresponded only to Cu_2S (Figure 3d). The results of additional TEM analysis of intermediate structures, in which Cu_2S and TiS_2 coexist, indicate that Cu_2S growth on the TiS_2 template occurs in a heteroepitaxial manner (Figure 3e, f). The interface between Cu_2S and TiS_2 forms a well-aligned hexagonal set of red and green spots for the (110) plane in the FFT (Figure 3f inset) with lattice fringes of 1.9 and 1.7 Å (Figure 3f). An EELS elemental scan analysis (Figure 3g−i) of a side view of the structure displays a dark contrast in the center of the structure representing Ti (green) in the TiS_2 layers and a surrounding lighter region representing Cu (red) from the outer rims of Cu_2S.

To provide a better understanding of the chemical processes of these morphological transformations, detailed TEM analyses on side views of the products isolated under various reaction conditions ($CuCl_2/TiS_2$ ratios of 0.5, 1, 2, and 4) were carried out. Upon introduction of a relatively small amount of Cu ion, ($CuCl_2/TiS_2$ ratio of 0.5), edge nucleation and growth of Cu_2S appear in the TEM images as gray contrast (pink in the color-coded image) (Figure 4b). The HRTEM view given in Figure 4g shows that heteroepitaxial growth of Cu_2S takes place on the edge of TiS_2, where a 3.3 Å (002) lattice fringe of Cu_2S is observed parallel to the 5.7 Å (001) fringe of the TiS_2 template. Clearly, these reactive peripheral positions of TiS_2 serve as selective nucleation and growth sites because of the higher surface energies of the edge faces of TiS_2.[11] As the $CuCl_2/TiS_2$ ratio is increased to 1, the thickness of TiS_2 template decreases from 10 to 6.5 nm, and the diameter decreases from 150 nm (the original size of the TiS_2 template) to 120 nm (Figure 4c). At the same time, the thickness of Cu_2S on the rim increases to 15 nm. As the amount of Cu ion is increased further, continued decrease in both the thickness and diameter of the TiS_2 template take place in concert with the growth of the Cu_2S rim (Figure 4d) until a pure toroidal Cu_2S structure is formed (Figure 4e). During the formation of the toroidal Cu_2S structure, indicated by white dashed lines in Figure 4c−e, the double-convex curvature of Cu_2S becomes apparent. The size changes that occur under the explored reaction conditions are summarized in Figure 4j. During these processes, heteroepitaxial growth continues to take place under the conditions described above, and well-defined interfacial fringes, including (001) of TiS_2 and (002), (102), and (104) of Cu_2S (Figure 4h), are clearly seen.

A side-view TEM image (Figure 4i) and the results of ED measurements (Figure 4l) show that the toroidal Cu_2S generated in the manner described above possesses single crystallinity with a well-defined (002) lattice fringe. The observations suggest that selective chemical exchange takes place on the edges of the 2D nanodiscs and that corresponding anion migration via nano-channels facilitates the shape transformation processes. Specifically, the reactive edges of the TiS_2 template are first nucleated with Cu_2S (Figure 4b′). Next, the interfacial exchange process involving Cu and Ti ions proceeds, and sulfur ions migrate through nanometer-sized channels. These events promote inward Cu_2S growth, eventually producing the double-convex curvature (Figure 4c′,c″,d′,d″,e′,e″). Importantly, the morphological changes observed in this process are clearly different from those involved in generating the concavo-convex hollow structures that have typically been observed in previous studies.[5]

dx.doi.org/10.1021/ja2049594 |J. Am. Chem. Soc. 2011, 133, 14500–14503

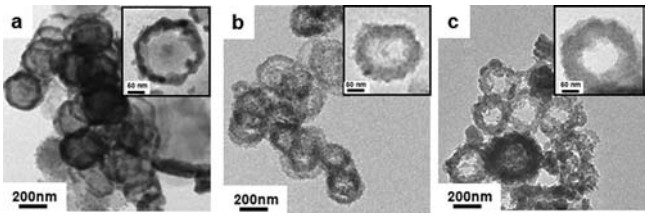

Figure 5. TEM images of toroidal-shaped nanostructures synthesized by reactions of TiS_2 discs with Ag, Mn, and Cd cations: (a) TiS_2-Ag_2S; (b) TiS_2-MnS; (c) CdS. The insets show higher-magnification images.

The principles of using 2D layered templates for building toroidal nanocrystals seem to be broadly applicable. We carried out reactions between TiS_2 and Ag, Mn, and Cd cations, which consistently resulted in similar toroidal intermediate nanostructures of TiS_2-Ag_2S and TiS_2-MnS and a fully converted toroid of CdS, respectively (Figure 5).

Since the first description of hollow nanocrystals involving the use of preformed nanocrystals as templates, research activities have been rapidly extended to produce various shapes and chemical compositions.[5,12,13] Nonetheless, the previous work has not been extended to 2D layered materials until now. Our findings of regioselective chemical reactivity and proposed mechanisms in the structural transformation of 2D layered nanocrystals are unprecedented. In addition, we have demonstrated that our approach can serve as a general protocol for the synthesis of inorganic toroidal nanocrystals. This study has not only provided new insight into the unique chemical reactivity of 2D layered nanomaterials but also revealed that the roles of edges and layers should be taken into account when considering the design and applications of 2D nanocrystals.

■ ASSOCIATED CONTENT

Supporting Information. Details of synthetic methods, elemental mapping, and XRD patterns. This material is available free of charge via the Internet at http://pubs.acs.org.

■ AUTHOR INFORMATION

Corresponding Author
jcheon@yonsei.ac.kr

■ ACKNOWLEDGMENT

This study was financially supported by the Creative Research Initiative (2010-0018286), WCU (2008-9-1955), BK21, and KBSI–HVEM (JEM–ARM 1300S). We thank M.-C. Kim and Professor E. Sim for surface energy calculations.

■ REFERENCES

(1) (a) Burda, C.; Chen, X.; Narayanan, R.; El-Sayed, M. A. *Chem. Rev.* **2005**, *105*, 1025. (b) Xia, Y.; Xiong, Y.; Lim, B.; Skrabalak, S. E. *Angew. Chem., Int. Ed.* **2009**, *48*, 60. (c) Mann, S. *Nat. Mater.* **2009**, *8*, 781. (d) Zecchina, A.; Bordiga, S.; Groppo, E. *Selective Nanocatalysts and Nanoscience: Concepts for Heterogeneous and Homogeneous Catalysis*, 1st ed.; Wiley-VCH: Weinheim, Germany, 2011.

(2) (a) Geim, A. K.; Novoselov, K. S. *Nature* **2007**, *6*, 183. (b) Tung, V. C.; Allen, M. J.; Yang, Y.; Kaner, R. B. *Nat. Nanotechnol.* **2009**, *4*, 25. (c) Park, S.; Ruoff, R. S. *Nat. Nanotechnol.* **2009**, *4*, 217. (d) Rao, C. N. R.; Sood, A. K.; Sood, A. K.; Subrahmanyam, K. S.; Govindaraj, A. *Angew. Chem., Int. Ed.* **2009**, *48*, 7752. (e) Bonaccorso, F.; Sun, Z.; Hasan, T.; Ferrari, A. C. *Nat. Photonics* **2010**, *4*, 611.

(3) (a) Dresselhaus, M. S. *Intercalation in Layered Materials*; NATO ASI Series; Plenum Press: New York, 1986. (b) Friend, R. H.; Yoffe, A. D. *Adv. Phys.* **1987**, *36*, 1. (c) Chen, J.; Tao, Z.-D.; Li, S.-L. *Angew. Chem., Int. Ed.* **2003**, *115*, 2197. (d) Seo, J.-w.; Jun, Y.-w.; Park, S.-w; Nah, H.; Moon, T.; Park, B.; Kim, J.-G.; Kim, Y. J.; Cheon, J. *Angew. Chem., Int. Ed.* **2007**, *46*, 8828. (e) Jang, J.-t.; Jeong, S.; Seo, J.-w.; Kim, M.-C.; Sim, E.; Oh, Y.; Nam, S.; Park, B.; Park, B.; Cheon, J. *J. Am. Chem. Soc.* **2011**, *133*, 7636. (f) Sekar, P.; Greyson, E. C.; Barton, J. E.; Odom, T. W. *J. Am. Chem. Soc.* **2005**, *127*, 2054. (g) Park, K. H.; Jang, K.; Son, S. U. *Angew. Chem. Int. Ed.* **2006**, *45*, 4608. (h) Radisavljevic, B.; Radenovic, A.; Brivio, J.; Giacometti, V.; Kis, A. *Nat. Nanotechnol.* **2011**, *6*, 147. (i) Coleman, J. N.; Lotya, M.; O' Neill, A.; Bergin, S. D.; King, P. J.; Khan, U.; Young, K.; Gaucher, A.; De, S.; Smith, R. J.; Shvets, I. V.; Arora, S. K.; Stanton, G.; Kim, H.-Y.; Lee, K.; Kim, G. T.; Duesberg, G. S.; Hallam, T.; Boland, J. J.; Wang, J. M.; Donegan, J. F.; Grunlan, J. C.; Moriarty, G.; Shmeliov, A.; Nicholls, R. J.; Perkins, J. M.; Grieveson, E. M.; Theuwissen, K.; McComb, D. W.; Nellist, P. D.; Nicolosi, V. *Science* **2011**, *331*, 568.

(4) (a) Kobayashi, Y.; Fukui, K.; Enoki, T.; Kusakabe, K. *Phys. Rev. B* **2006**, *73*, 125415. (b) Jaramillo, T. F.; Jorgensen, , K. P.; Bonde, J.; Nielsen, J. H.; Horch, S.; Chorkendorff, I. *Science* **2007**, *317*, 100. (c) Cervantes-Sodi, F.; Csanyi, G.; Piscanec, S.; Ferrari, A. *C. Phys. Rev. B* **2008**, *77*, 165427. (d) Suenaga, K.; Koshino, M. *Nature* **2010**, *468*, 1088.

(5) (a) Yin, Y.; Rioux, R. M.; Erdonmez, C. K.; Hughes, S.; Somorjai, G. A.; Alivisatos, A. P. *Science* **2004**, *304*, 711. (b) Yin, Y.; Erdonmez, C. K.; Hughes, S.; Alivisatos, A. P. *Adv. Funct. Mater.* **2006**, *16*, 1389. (c) Fan, H. J.; Knez, M.; Scholz, R.; Nielsch, K.; Pippel, E.; Hesse, D.; Zacharias, M.; Gösele, U. *Nat. Mater.* **2006**, *5*, 627. (d) Peng, H.; Xie, C.; Schoen, D. T.; McIlwrath, K.; Zhang, X. F.; Cui, Y. *Nano Lett.* **2007**, *7*, 3734. (e) Park, J.; Zheng, H.; Jun, Y.-w.; Alivisatos, A. P. *J. Am. Chem. Soc.* **2009**, *131*, 13943. (f) Macdonald, J. E.; Sadan, M. B.; Houben, L.; Popov, I.; Banin, U. *Nat. Mater.* **2010**, *9*, 810.

(6) (a) Haft, D.; Schulhauser, C.; Govorov, A. O.; Warburton, R. J.; Karral, K.; Garcìa, J. M.; Schoenfeld, W.; Petroff, P. M. *Physica E* **2002**, *13*, 165. (b) Aizpurua, J.; Hanarp, P.; Sutherland, D. S.; Käll, M.; Bryant, G. W.; Abajo, F. J. G. D. *Phys. Rev. Lett.* **2003**, *90*, No. 057401. (c) Kippenberg, T. J; Spillane, S. M.; Vahala, K. *J. Phys. Rev. Lett.* **2004**, *93*, 083904.

(7) (a) Ross, C. A.; Castano, F. J.; Morecroft, D.; Jung, W.; Smith, I. H.; Moore, T. A.; Hayward, T. J.; Bland, J. A. C.; Bromwich, T. J.; Petford-Long, A. K. *J. Appl. Phys.* **2006**, *99*, No. 08S501. (b) Gao, X. S.; Adeyeye, A. O.; Goolaup, S.; Singh, N.; Jung, W.; Castano, F. J.; Ross, C. A. *J. Appl. Phys.* **2007**, *101*, No. 09F505.

(8) (a) Lu, G.; Li, W.; Yao, J.; Zhang, G.; Yang, B.; Shen, J. *Adv. Mater.* **2002**, *14*, 1049. (b) Balzer, F.; Beermann, J.; Bozhevolnyi, S. I.; Simonsen, A. C.; Rubahn, H.-G. *Nano Lett.* **2003**, *3*, 1311. (c) Zhang, X.; Choi, H. S.; Armani, A. M. *App. Phys. Lett.* **2010**, *96*, 153304. (d) Lin, S.; Schonbrun, E.; Crozier, K. *Nano Lett.* **2010**, *10*, 2408.

(9) (a) McLellan, J. M.; Geissler, M.; Xia, Y. *J. Am. Chem. Soc.* **2004**, *126*, 10830. (b) Hobbs, K. L.; Larson, P. R.; Lian, G. D.; Keay, J. C.; Johnson, M. B. *Nano Lett.* **2004**, *4*, 167. (c) Lee, E.; Kim, J.-K.; Lee, M. *J. Am. Chem. Soc.* **2009**, *131*, 18242.

(10) TiS_2, JCPDS no. 15-0853; Cu_2S, ICSD no. 16242.

(11) (a) Tenne, R. *Angew. Chem., Int. Ed.* **2003**, *42*, 5124. (b) According to the results of ab initio calculations, the surface energies of edge faces, such as (100) or (101), of TiS_2 are ~4.5 times larger than that of the planar face (001).

(12) (a) Huang, X.; Zhang, H.; Guo, C.; Zhou, Z.; Zheng, N. *Angew. Chem., Int. Ed.* **2009**, *48*, 4808. (b) Seo, D.; Song, H. *J. Am. Chem. Soc.* **2009**, *131*, 18210. (c) Wang, Z.; Luan, D.; Li, C. M.; Su, F.; Madhavi, S.; Boey, F. Y. C.; Lou, X. W. *J. Am. Chem. Soc.* **2010**, *132*, 16271. (d) Korhonen, J. T.; Hiekkataipale, P.; Malm, J.; Karppinen, M.; Ikkala, O.; Ras, R. H. A. *ACS Nano* **2011**, *5*, 1967.

(13) Shevchenko, E.; Bodnarchuck, M. I.; Kovalenko, M. V.; Talapin, D. V.; Smith, R. K.; Aloni, S.; Heiss, W.; Alivisatos, A. P. *Adv. Mater.* **2008**, *20*, 4323.